

Electronic Supplementary Information

Reactivity of a half-lantern Pt₂(II,II) complex with triphenylphosphine: Selectivity in protonation reaction

Maryam Niazi,^a Hamid R. Shamsavari,^{a} Mohsen Golbon Haghighi,^b Mohammad Reza Halvagar,^c Samaneh Hatami^a and Behrouz Notash^b*

^aDepartment of Chemistry, Institute for Advanced Studies in Basic Sciences (IASBS), Yousef Sobouti Blvd., Zanzan 45137-6731, Iran.

^bDepartment of Chemistry, Shahid Beheshti University, Evin, Tehran 1983963113, Iran

^cChemistry & Chemical Engineering Research Center of Iran, Tehran, 14968-13151, Iran

Email: shamsavari@iasbs.ac.ir

Contents:	Page
Table S1. Composition (%) of frontier MOs for complex 2 in acetone solution.	3
Table S2. TD-DFT computed and experimental wavelengths (nm) for the lower energy band in complex 2 in acetone solution.	3
Figure S1. ^1H NMR spectra of complex (a) 1a and (b) reaction mixture of complex 1a with PPh_3 in CD_2Cl_2 at room temperature.	4
Figure S2. ^{31}P $\{^1\text{H}\}$ NMR spectra of reaction mixture of complex 1a with PPh_3 in CD_2Cl_2 at room temperature and formed triphenylphosphine oxide.	5
Figure S3. Change in the absorbance spectra of complex $[\{\text{Pt}(\text{ppy})(\mu_2\text{-Spy})\}_2]$, 1 , with an excess of PPh_3 in acetone at $T = 25\text{ }^\circ\text{C}$ as function of wavelength; successive spectra recorded at intervals of 3 min.	6
Figure S4. Representative frontier orbitals involved in the absorption of complex 2 .	7
Figure S5. ESI-Mass spectrum of complex 2 in cationic mode.	8
Figure S6. ESI-Mass spectrum of complex 2 , peak corresponding to $[\text{Pt}(\text{ppy})(\eta^1\text{-Spy})(\text{PPh}_3)]^+$, $[\mathbf{2}]^+$ (experimental, black; simulated, blue).	9
Figure S7. ^{31}P $\{^1\text{H}\}$ NMR spectrum of complex 2 in CD_2Cl_2 at room temperature.	10
Figure S8. Complex 2 as monitored by ^{31}P $\{^1\text{H}\}$ NMR spectroscopy in $\text{dms}\text{-}d_6$ at room temperature. (a) complex 2 , (b) after 6h in the dry and deoxygenated solvent; (c) 6 h (d) 12 h, (e) 24 h and (f) 48 h in the hydrated (hydrous and aerated) solvent. The signal assignments are depicted.	11
Figure S9. Complex 2 as monitored by ^1H NMR spectroscopy in $\text{dms}\text{-}d_6$ at room temperature. (a) complex 2 , (b) 6 h, (c) 12 h, (d) 24 h, (e) 48 h, (f) 72 h in the hydrous and aerated solvent and (g) complex 1 .	12
Figure S10. Photograph of transformation of complex 2 to complex 1 .	13
Figure S11. ^{31}P $\{^1\text{H}\}$ NMR spectra of (a) complex 2 and (b) complex 5 in acetone- d_6 at room temperature.	14
Figure S12. ^1H NMR spectra of (a) complex 2 and (b) complex 5 in acetone- d_6 at room temperature.	15
Figure S13. ^1H NMR spectra of (a) complex 5 (b) complex 5 + D_2O in acetone- d_6 at room temperature.	16
Table S3. Crystallographic and structure refinement data for complex 4 .	17
Figure S14. $\text{C-H}\cdots\pi$ interaction between C-H group adjacent to metalated carbon atom of the ppy ligand and the phenyl ring of PPh_3 ligand in complex 4 (green lines).	18
Figure S15. Intramolecular $\pi\cdots\pi$ contact between the SPh and phenyl ring of PPh_3 in complex 4 .	18

Table S1. Composition (%) of frontier MOs for complex **2** in acetone solution.

MO	Energies(ev)	Pt	Spy	ppy	PPh ₃
LUMO+4	-0.73	1	2	2	95
LUMO+3	-0.95	9	5	20	66
LUMO+2	-1.01	5	2	71	22
LUMO+1	-1.06	25	3	11	61
LUMO	-1.72	6	2	86	6
HOMO	-5.22	12	80	6	2
HOMO-1	-5.88	34	24	40	2
HOMO-2	-6.17	68	11	14	7
HOMO-3	-6.35	15	36	46	3
HOMO-4	-6.54	8	25	61	6

Table S2. TD-DFT computed and experimental wavelengths (nm) for the lower energy band in complex **2** in acetone solution.

λ_{cal} (nm)	f^{a}	λ_{exp} (nm)	Transition (Percentage Contribution)	Character	Assignment L = ppy, L' = Spy
433	0.018	420	HOMO→LUMO (70%)	d(Pt)/ π (spy)→ π^* (ppy)	¹ L'LCT/ ¹ MLCT

^a Oscillator strength

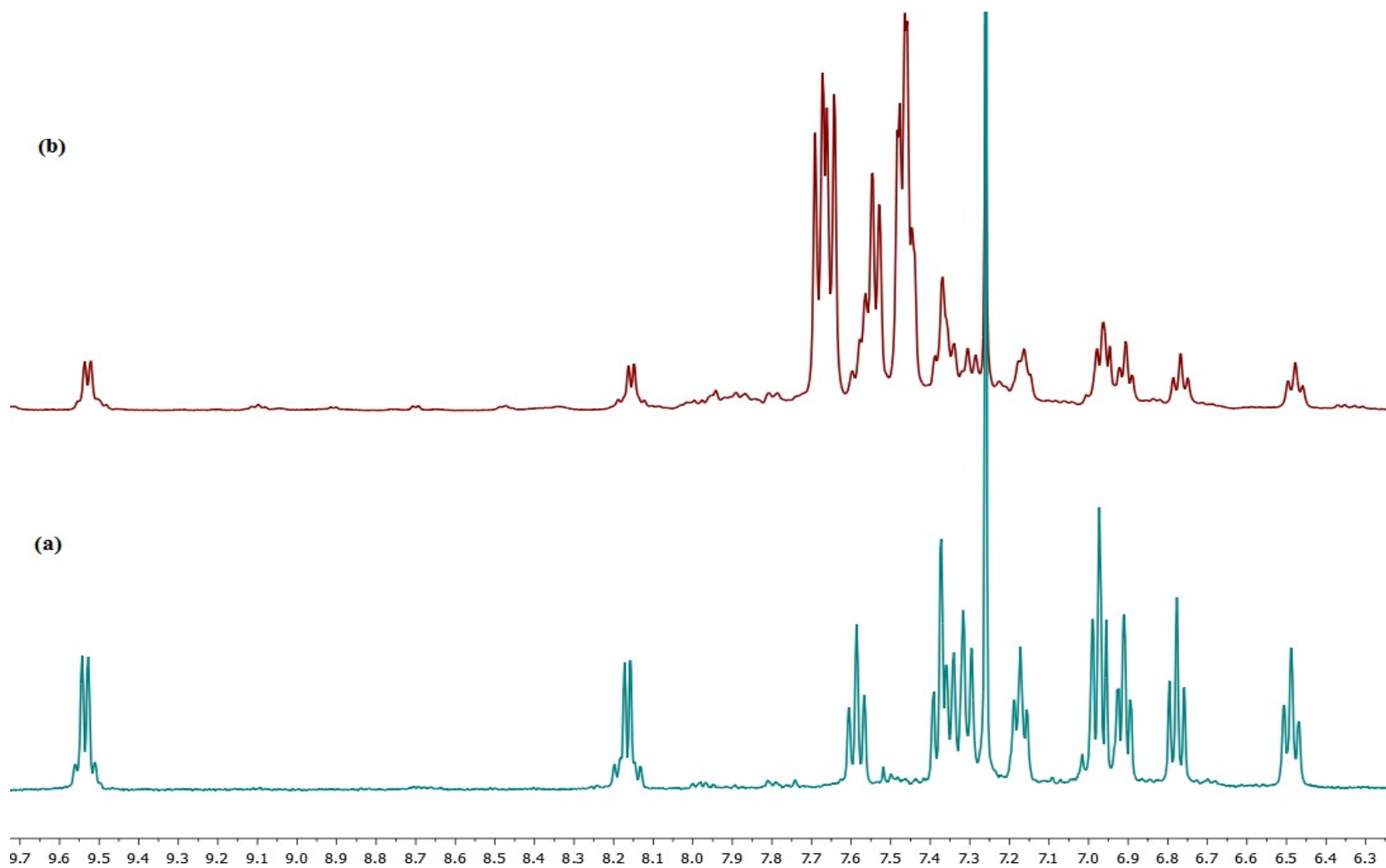


Figure S1. ¹H NMR spectra of complex (a) **1a** and (b) reaction mixture of complex **1a** with PPh₃ in CD₂Cl₂ at room temperature.

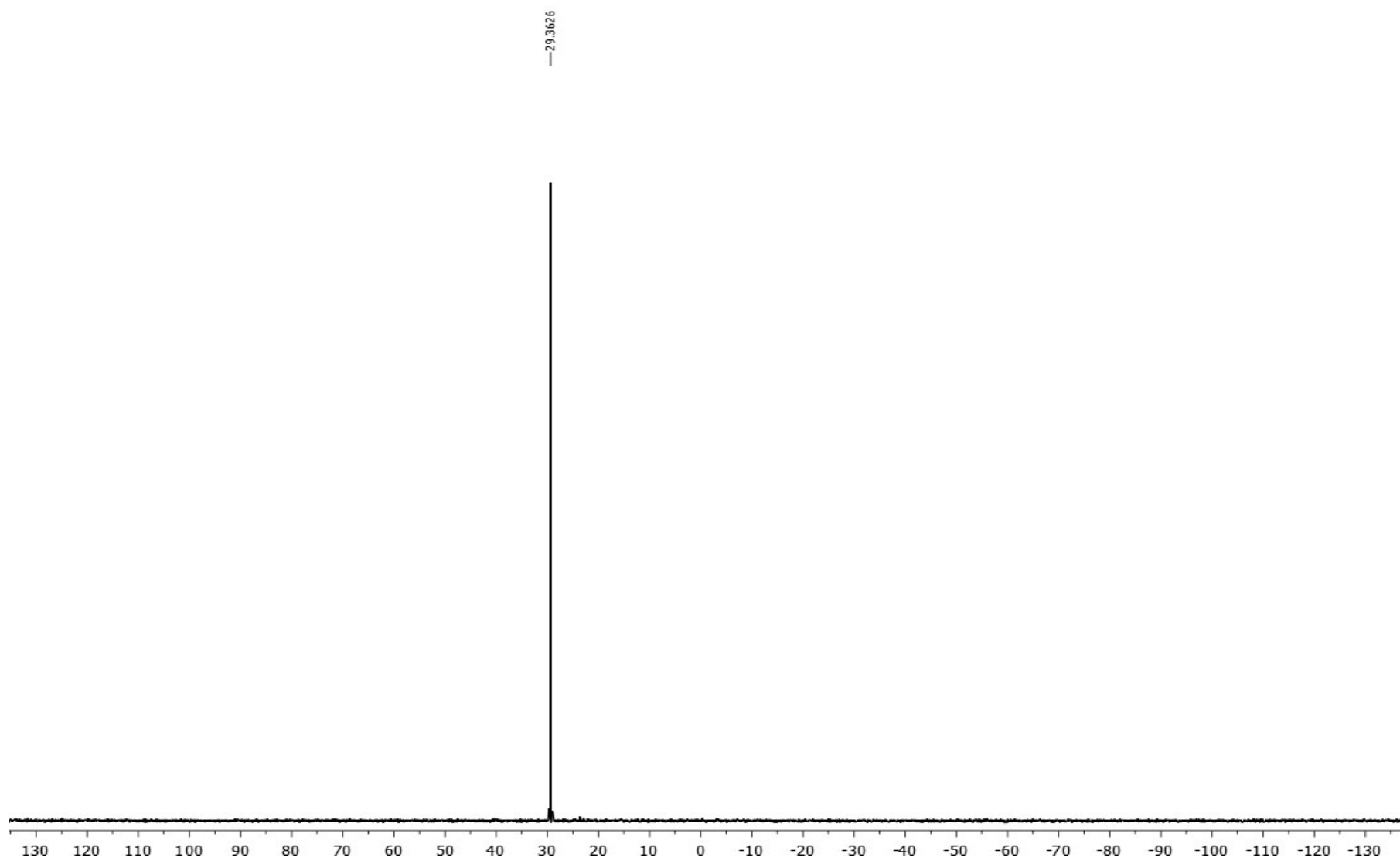


Figure S2. ^{31}P $\{^1\text{H}\}$ NMR spectra of reaction mixture of complex **1a** with PPh_3 in CD_2Cl_2 at room temperature and formed triphenylphosphine oxide.

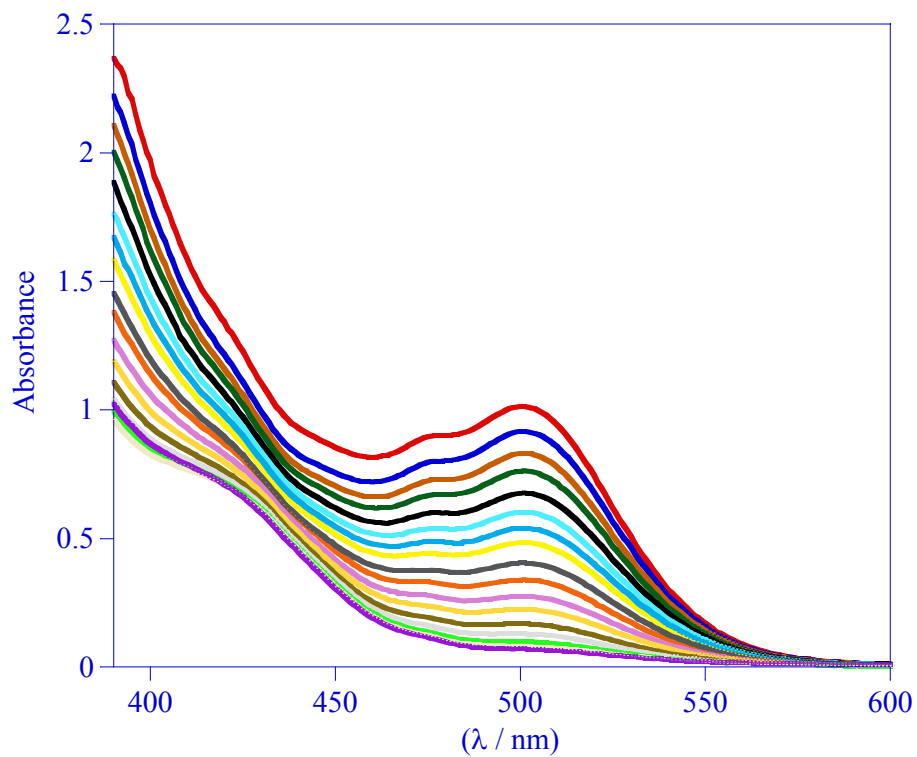


Figure S3. Change in the absorbance spectra of complex $[\{\text{Pt}(\text{ppy})(\mu_2\text{-Spy})\}_2]$, **1**, with an excess of PPh_3 in acetone at $T = 25\text{ }^\circ\text{C}$ as function of wavelength; successive spectra recorded at intervals of 3 min.

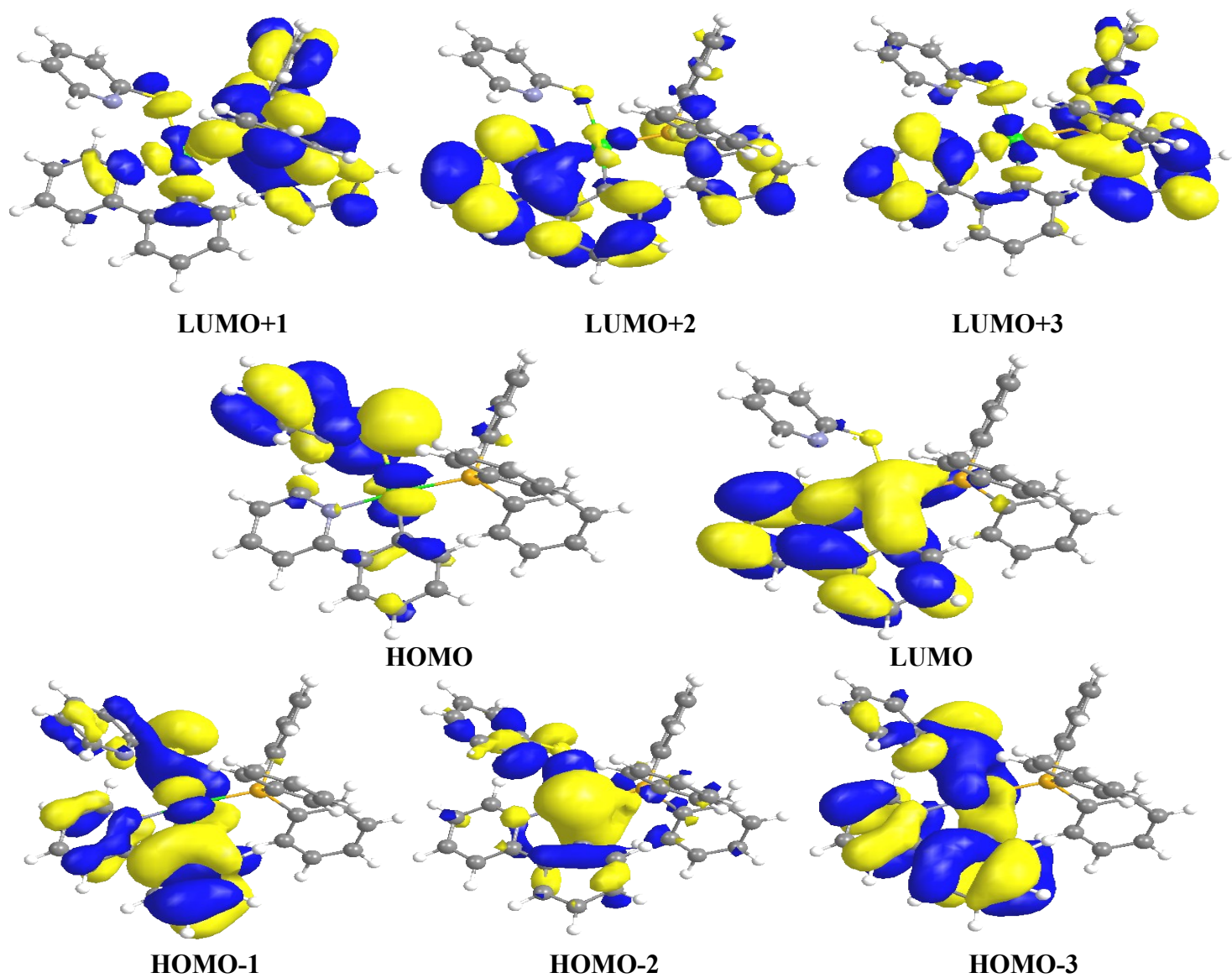


Figure S4. Representative frontier orbitals involved in the absorption of complex 2.

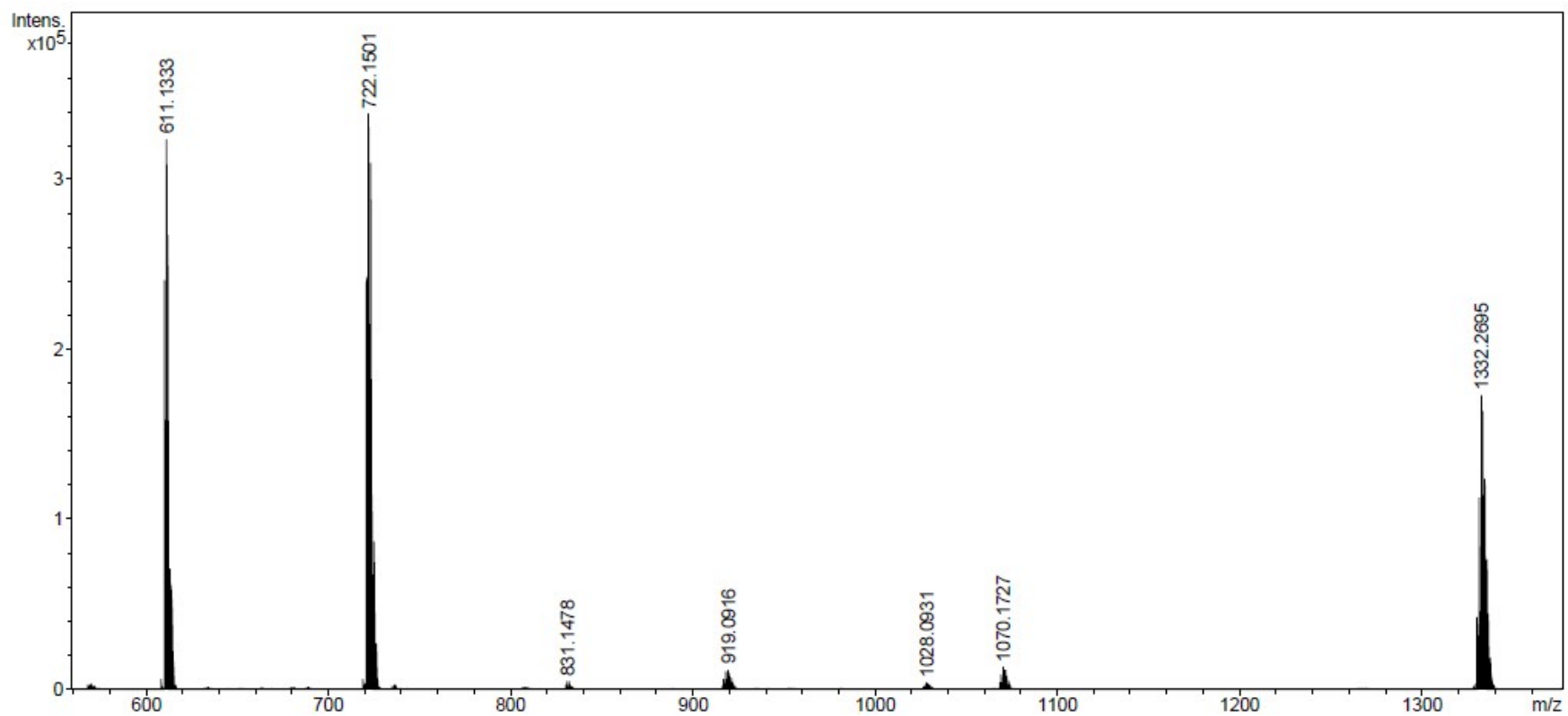


Figure S5. ESI-Mass spectrum of complex **2** in cationic mode.

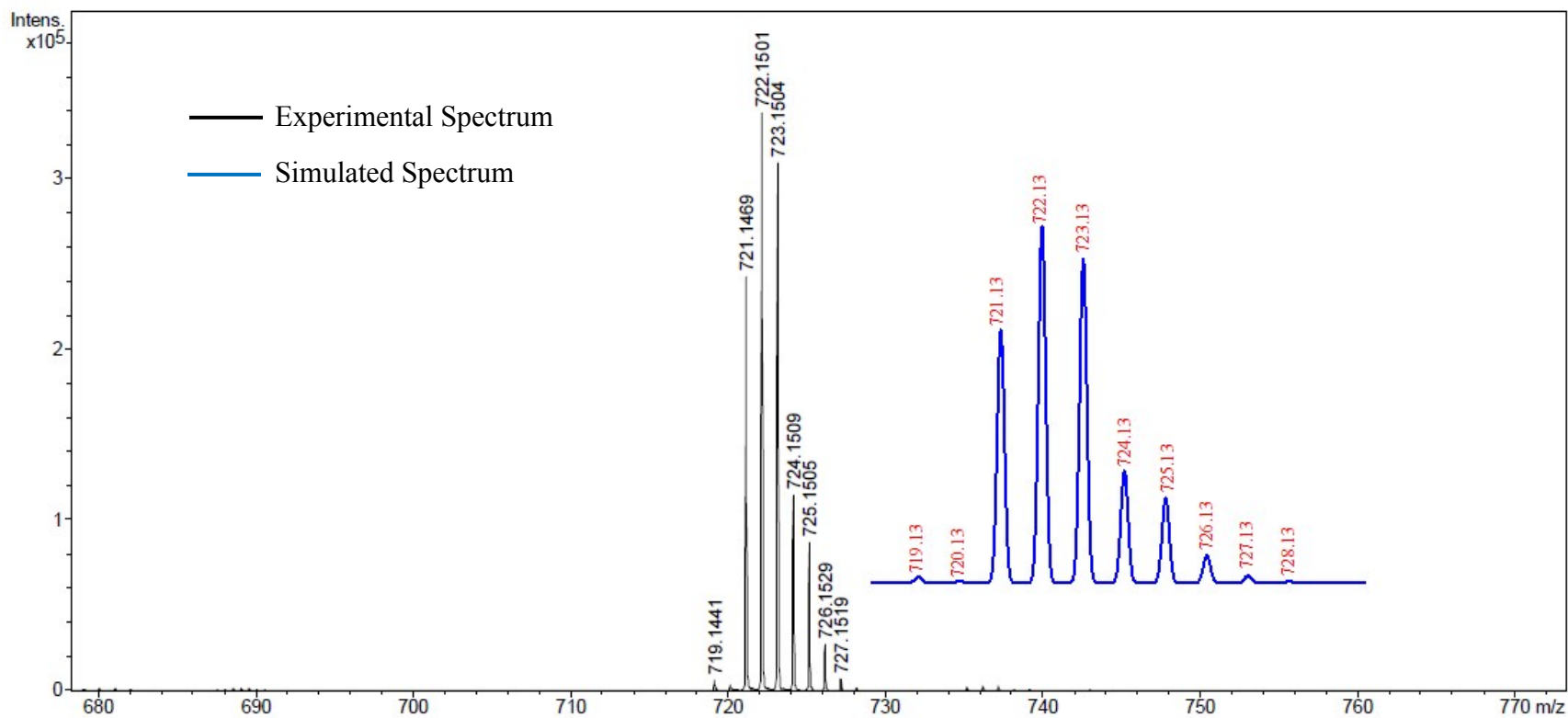


Figure S6. ESI-Mass spectrum of complex **2**, peak corresponding to $[\text{Pt}(\text{ppy})(\eta^1\text{-S-Spy})(\text{PPh}_3)]^+$, $[\mathbf{2}]^+$ (experimental, black; simulated, blue).

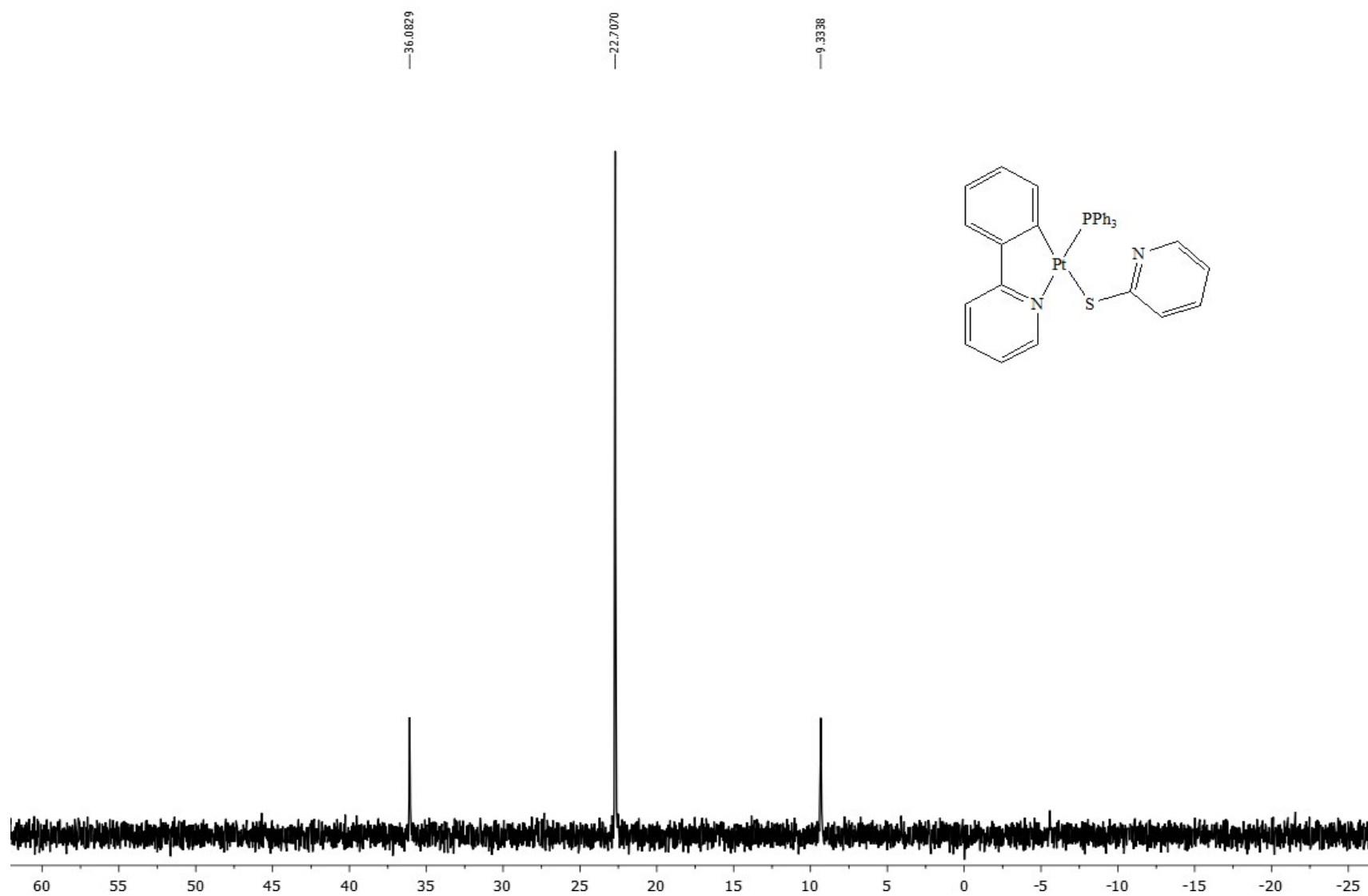


Figure S7. ^{31}P $\{^1\text{H}\}$ NMR spectrum of complex **2** in CD_2Cl_2 at room temperature.

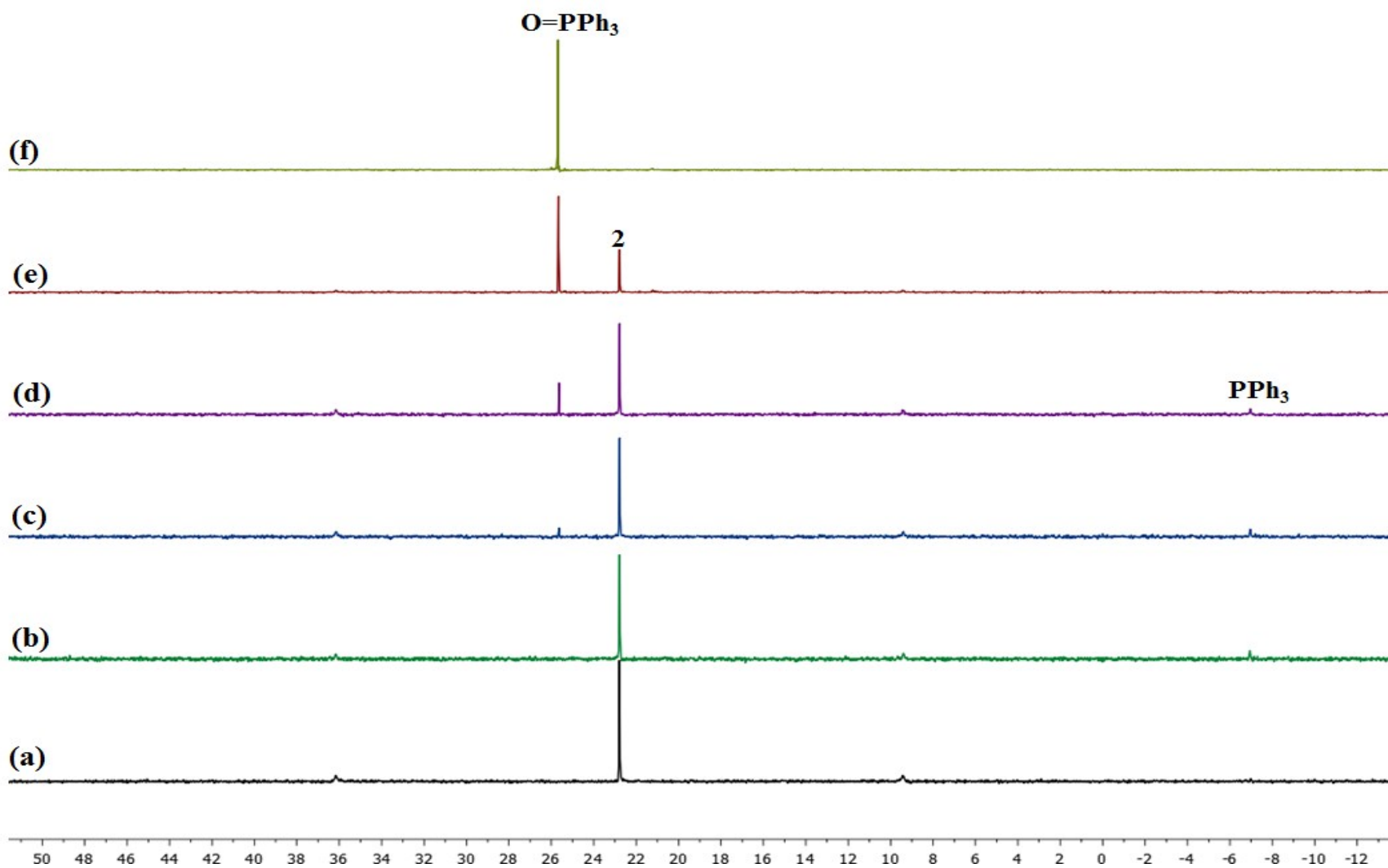


Figure S8. Complex **2** as monitored by ^{31}P $\{^1\text{H}\}$ NMR spectroscopy in $\text{dmsO-}d_6$ at room temperature. (a) complex **2**, (b) after 6h in the dry and deoxygenated solvent; (c) 6 h (d) 12 h, (e) 24 h and (f) 48 h in the hydrated (hydrous and aerated) solvent. The signal assignments are depicted.

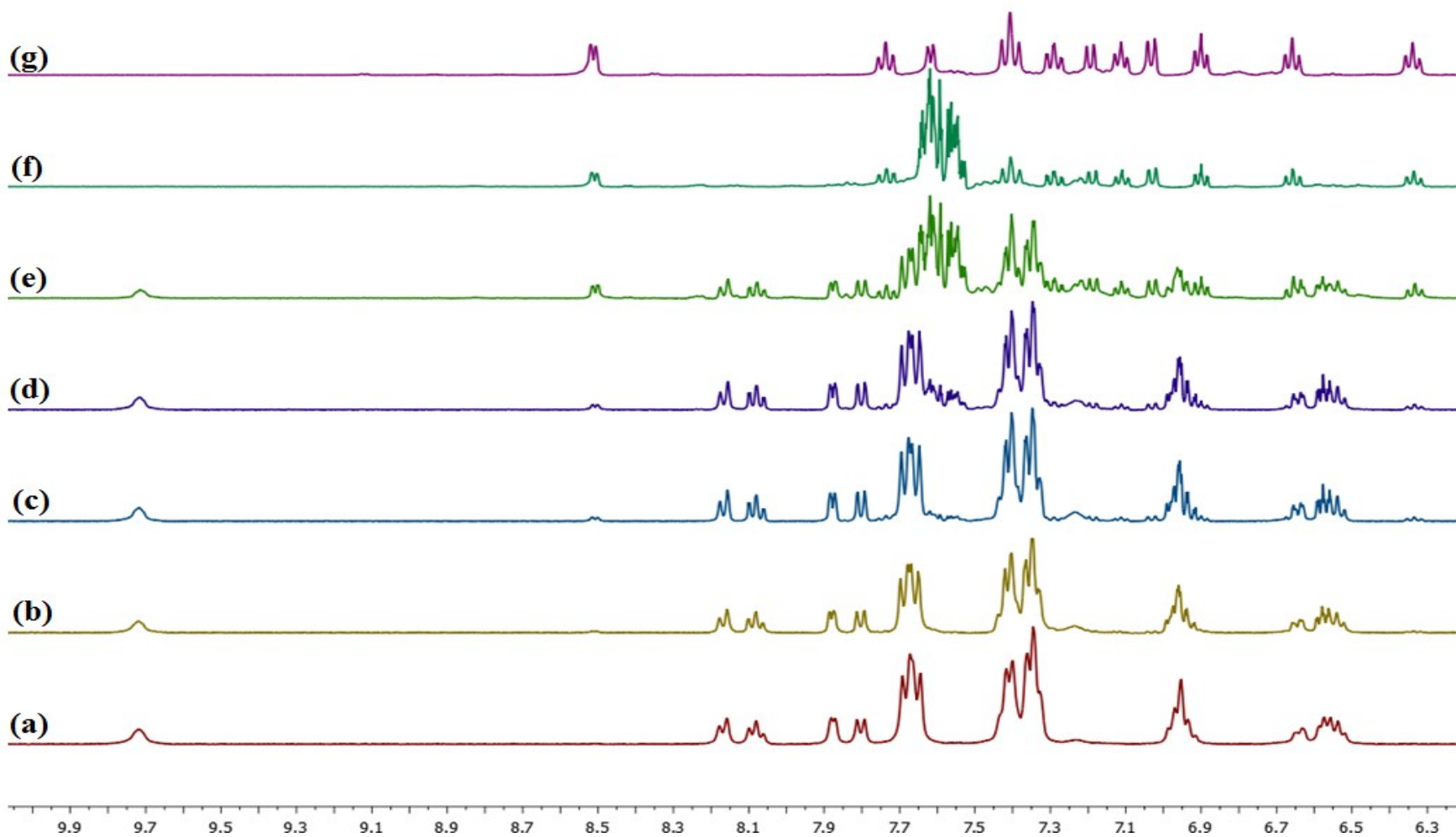


Figure S9. Complex **2** as monitored by ¹H NMR spectroscopy in dms0-*d*₆ at room temperature. (a) complex **2**, (b) 6 h, (c) 12 h, (d) 24 h, (e) 48 h, (f) 72 h in the hydrous and aerated solvent and (g) complex **1**.

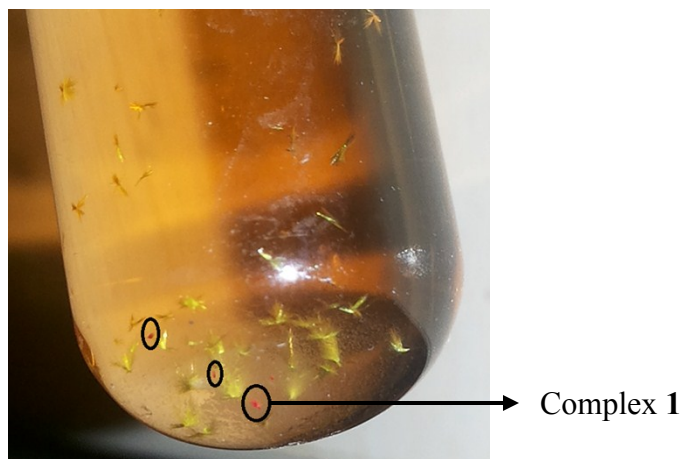


Figure S10. Photograph of transformation of complex 2 to complex 1.

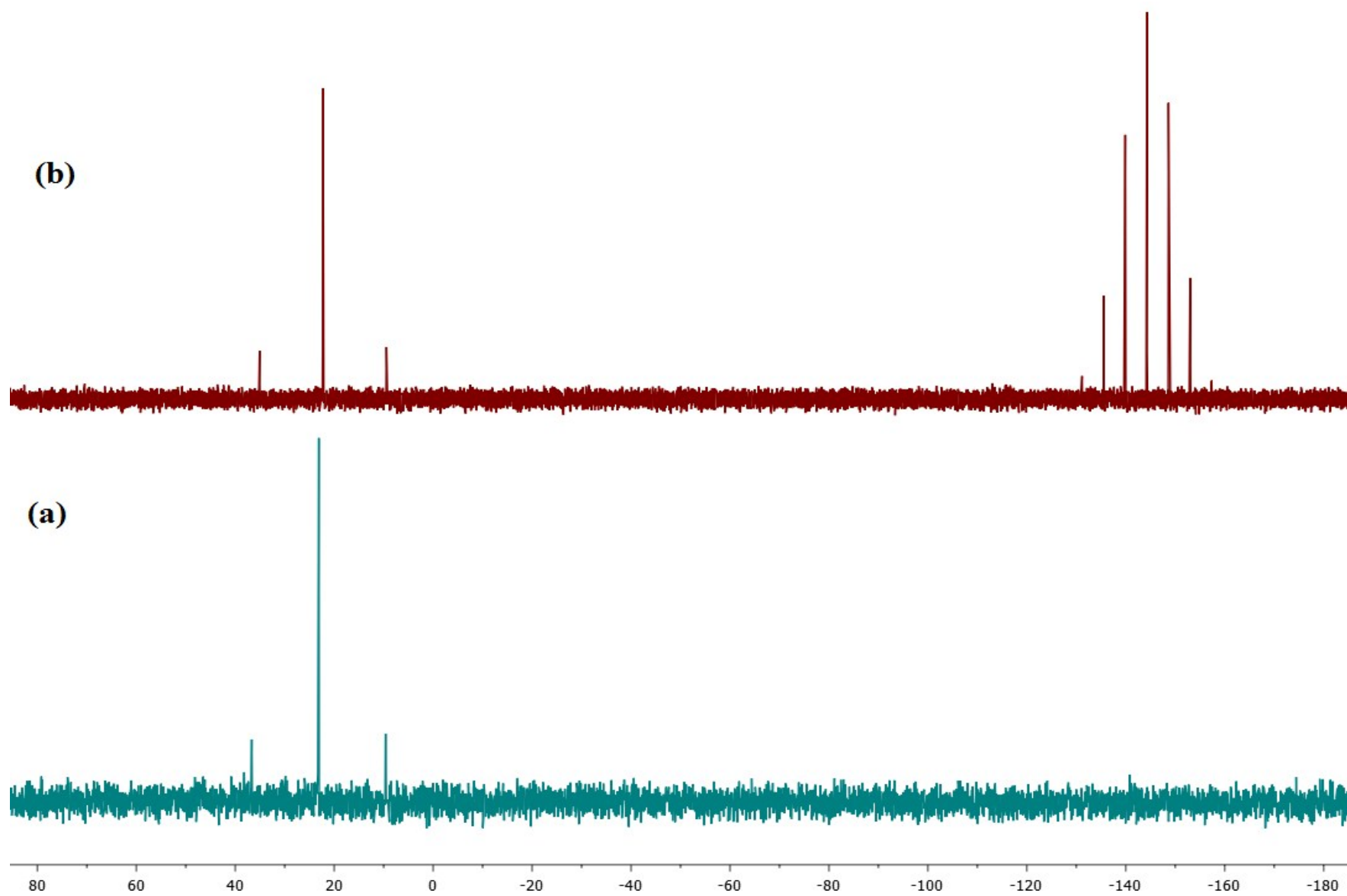


Figure S11. ^{31}P $\{^1\text{H}\}$ NMR spectra of (a) complex **2** and (b) complex **5** in acetone- d_6 at room temperature.

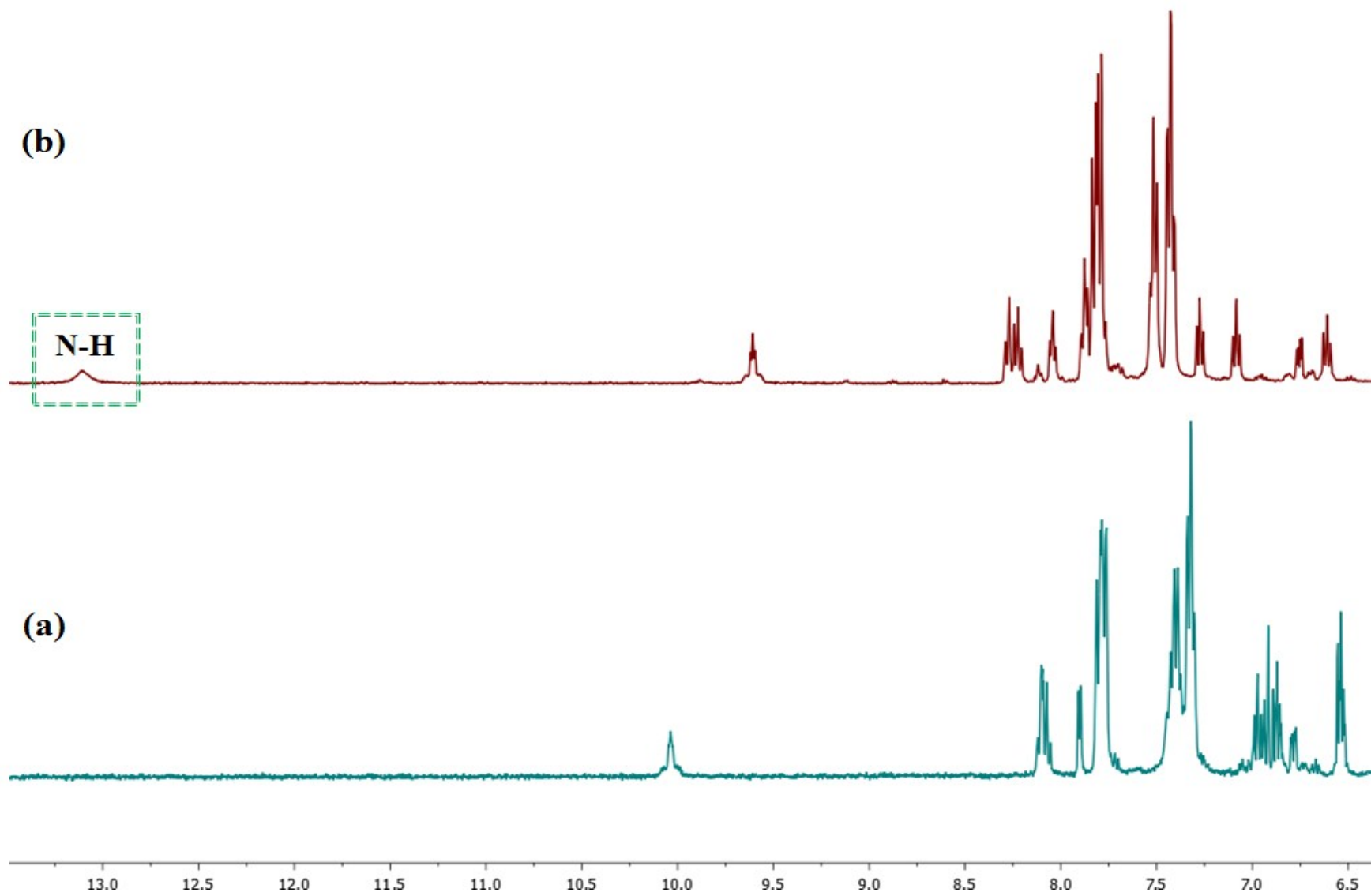


Figure S12. ¹H NMR spectra of (a) complex **2** and (b) complex **5** in acetone-*d*₆ at room temperature.

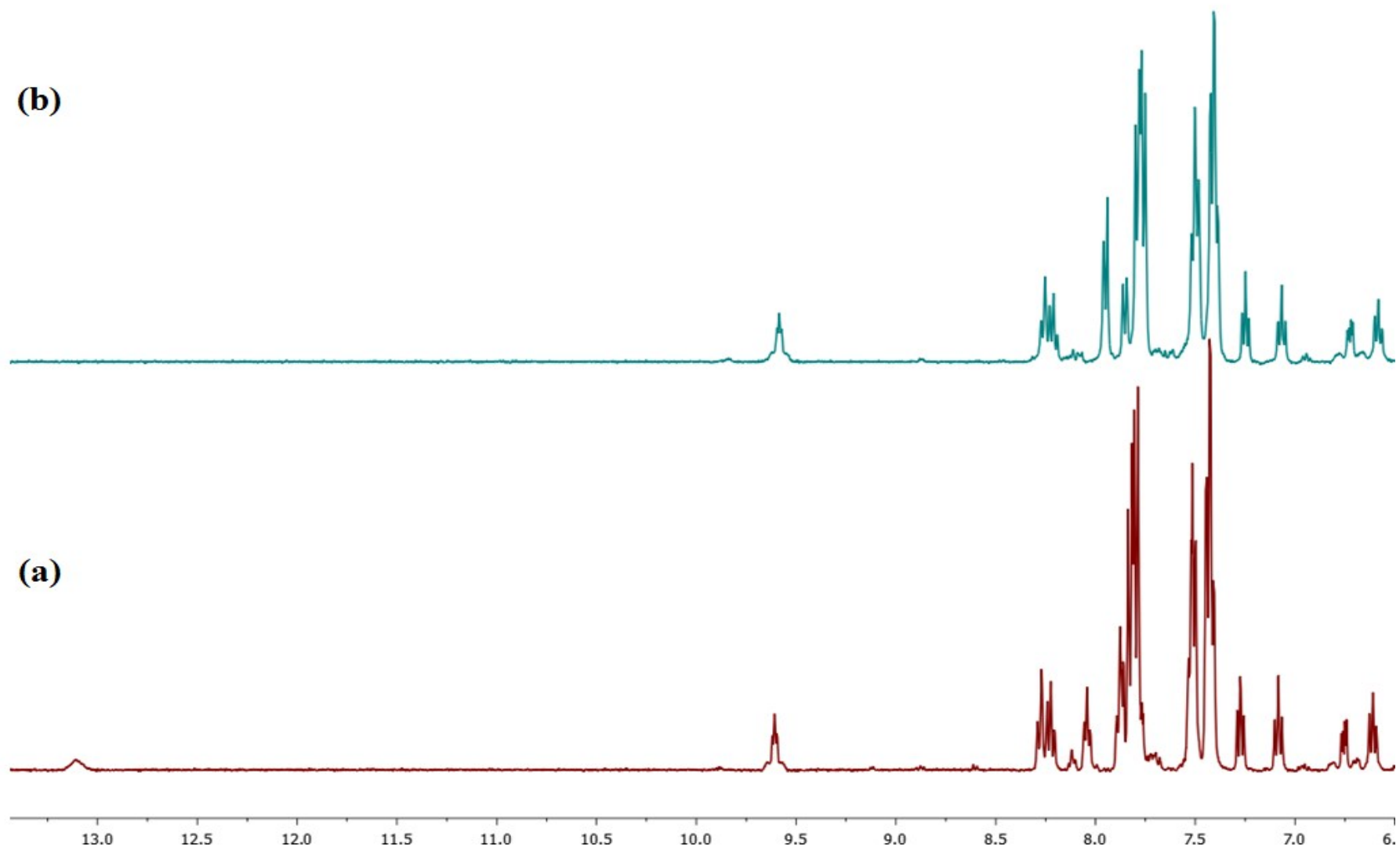


Figure S13. ¹H NMR spectra of (a) complex **5** (b) complex **5** + D₂O in acetone-*d*₆ at room temperature.

Table S3. Crystallographic and structure refinement data for complex **4**.

Formula	C ₃₅ H ₂₈ NPtS
Formula weight	720.69
T (K)	298(2)
λ (Å)	0.71073
Crystal system	Monoclinic
Space Group	<i>P2</i> ₁ / <i>c</i>
Crystal size(mm)	0.25×0.15×0.12
<i>a</i> (Å)	17.452(4)
<i>b</i> (Å)	8.2580(17)
<i>c</i> (Å)	20.121(4)
α (°)	90
β (°)	90.95(3)
γ (°)	90
<i>V</i> (Å ³)	2899.4(10)
<i>Z</i>	4
<i>D</i> _{calc} (g cm ⁻³)	1.651
θ_{\min} , θ_{\max} (°)	2.32-25.00
<i>F</i> ₀₀₀	1416
μ (mm ⁻¹)	4.992
Index ranges	-20 ≤ <i>h</i> ≤ 20 -9 ≤ <i>k</i> ≤ 9 -23 ≤ <i>l</i> ≤ 23
Data collected	15434
Unique data	5090
<i>R</i> ₁ ^a , <i>wR</i> ₂ ^b (<i>I</i> > 2 σ (<i>I</i>))	0.0542, 0.1014
<i>R</i> ₁ ^a , <i>wR</i> ₂ ^b (all data)	0.1170, 0.1142
GOF on <i>F</i> ² (<i>S</i>)	0.803

$$^a R_1 = \frac{\sum ||F_o| - |F_c||}{\sum |F_o|}, \quad ^b wR_2 = \left[\frac{\sum (w(F_o^2 - F_c^2)^2)}{\sum w(F_o^2)^2} \right]^{1/2}$$

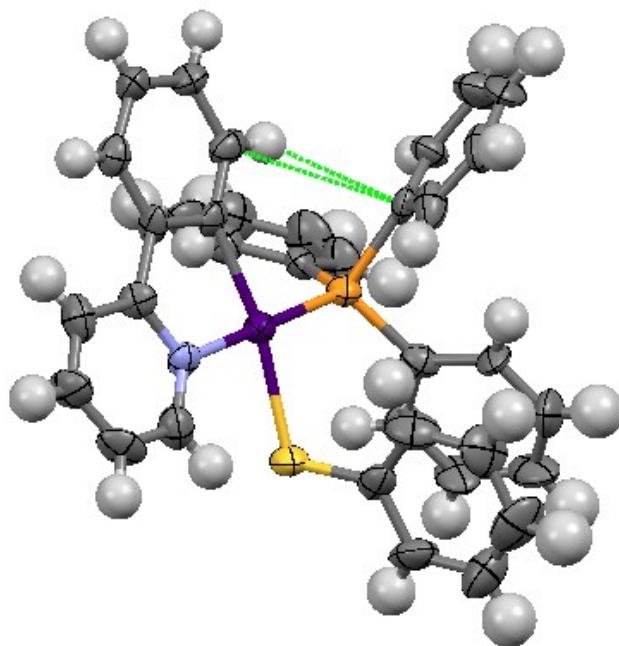


Figure S14. C–H $\cdots\pi$ interaction between C–H group adjacent to metalated carbon atom of the ppy ligand and the phenyl ring of PPh₃ ligand in complex **4** (green lines).

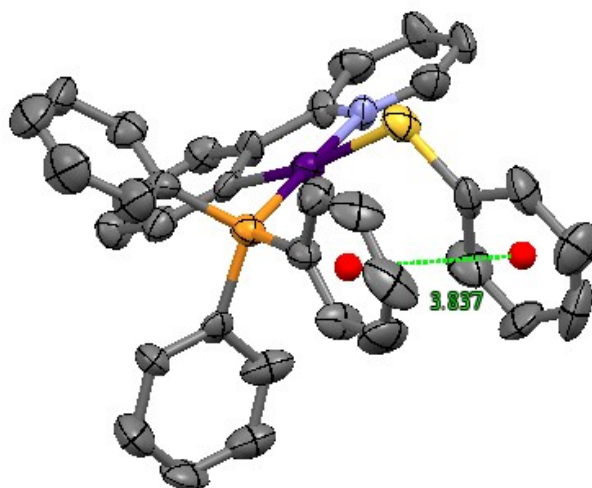


Figure S15. Intramolecular $\pi\cdots\pi$ contact between the SPh and phenyl ring of PPh₃ in complex **4**.